Electronic Supplementary Material (ESI) for Journal of Materials Chemistry A.

Supporting information

Unraveling promotional role of $BaCO_3$ on the electrode reaction kinetics of $SmBaFe_2O_{5+\delta}$ air electrode of reversible solid oxide cells

Min Zhang,[a] *Zhihong Du,*[a,b] *Zhipeng Sun,*[a] *Hailei Zhao*,*[a,b]

a School of Materials Science and Engineering, University of Science and Technology Beijing, Beijing, 100083, China

b Beijing Municipal Key Lab for Advanced Energy Materials and Technologies, Beijing, 100083, China

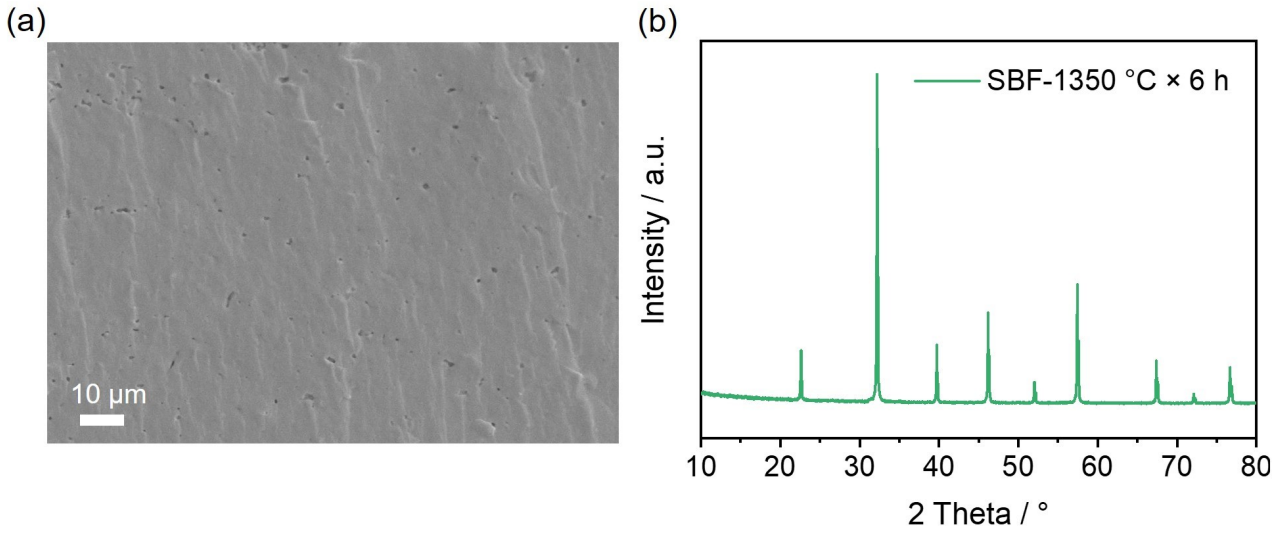

Fig. S1. Cross-section SEM image (a) and XRD pattern of SBF bar for TEC and electrical conductivity measurement after sintering at 1350 °C for 6 h.

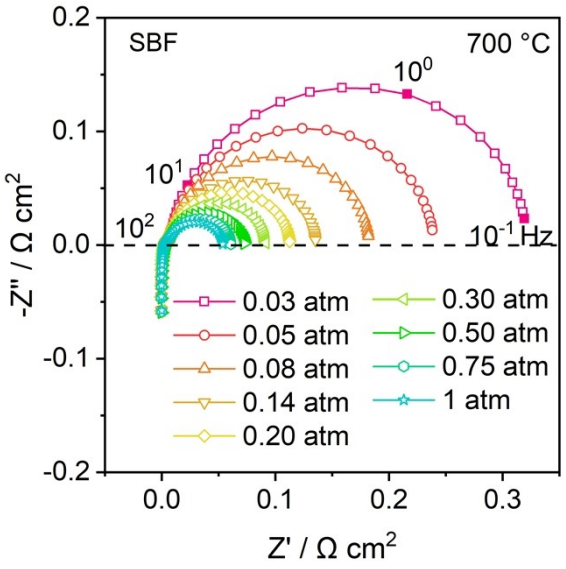

Fig. S2. Nyquist plots of a symmetrical cell with LSGM electrolyte and SBF electrode measured under different oxygen partial pressures at 700 °C.

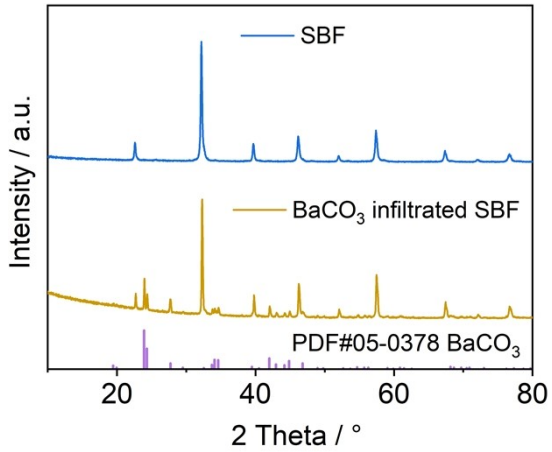

Fig. S3. XRD pattens of pristine SBF and $BaCO_3$ infiltrated SBF electrode after calcining at 650 °C in air.

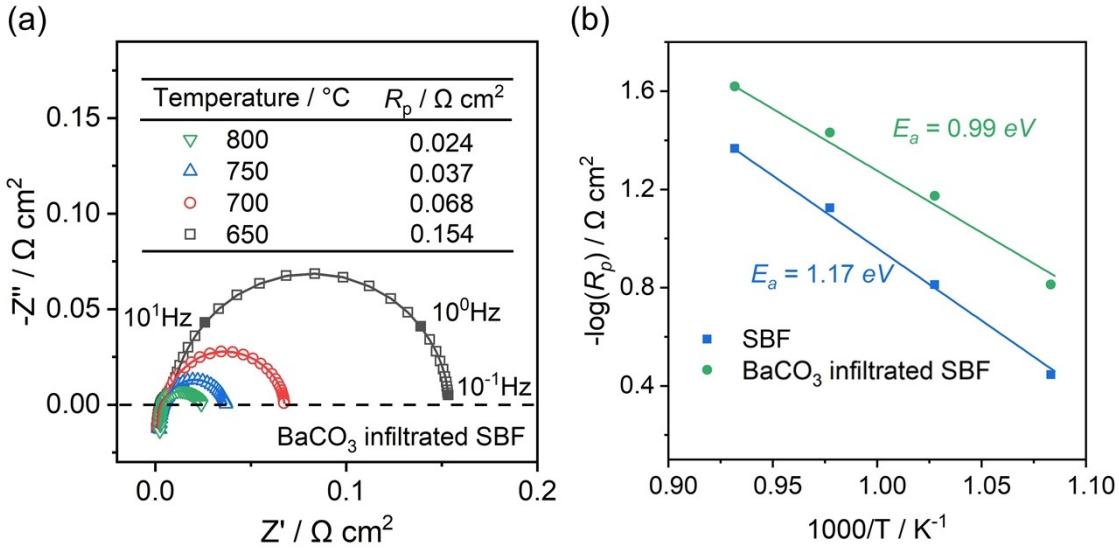

Fig. S4. (a) EIS of $BaCO_3$ infiltrated SBF air electrode recorded in temperature range of 650-800 °C in air. (b) Arrhenius plots of polarization resistance of pristine SBF (based on the data shown in Fig. 2a) and $BaCO_3$ infiltrated SBF electrodes.

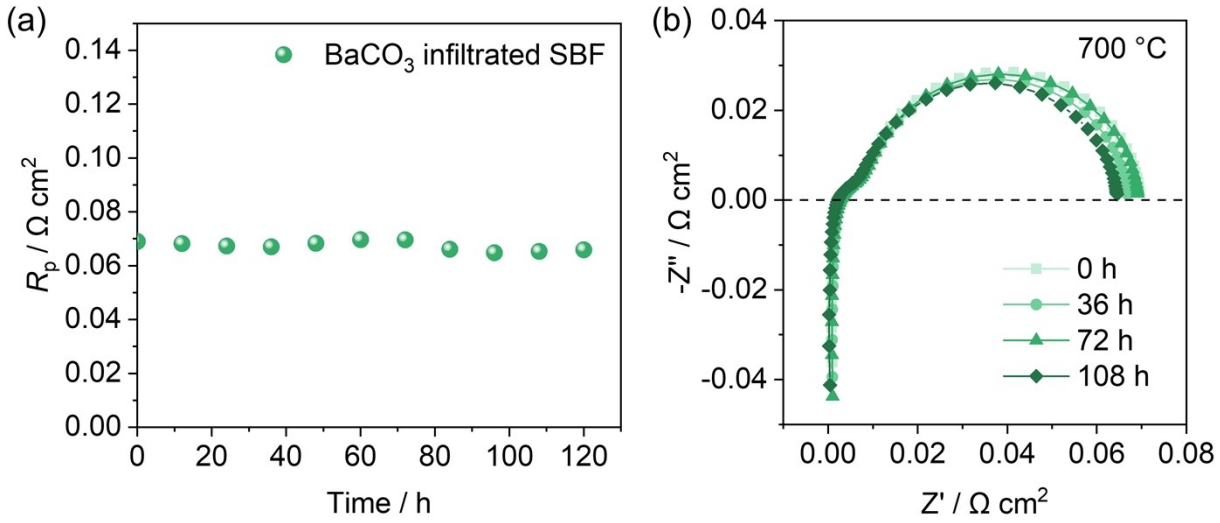

Fig. S5. (a) Polarization resistance and (b) Nyquist plots of symmetrical cell with $BaCO_3$ infiltrated SBF electrodes during short-term test at 700 °C in air.

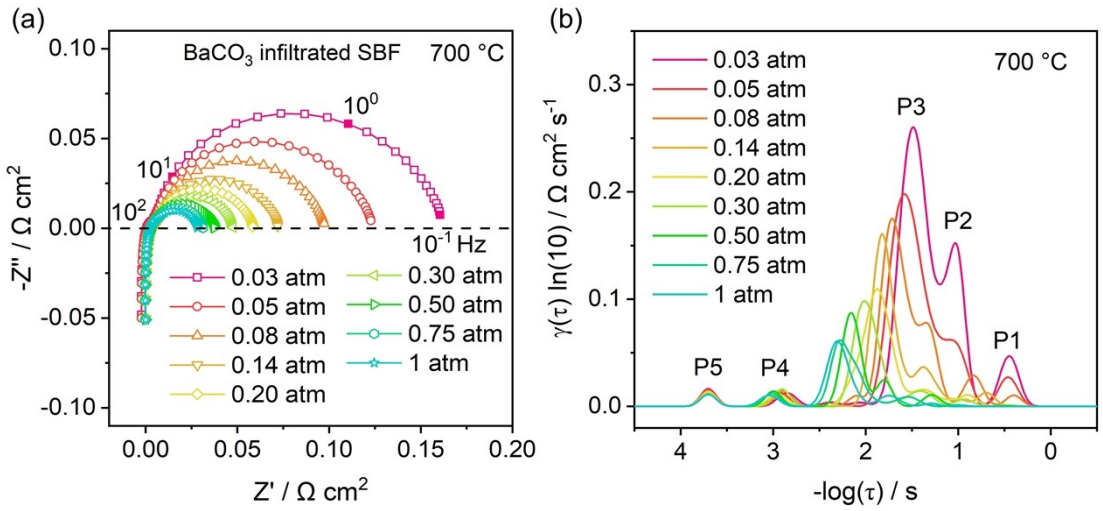

Fig. S6. Nyquist plots (a) and DRT spectra (b) of a symmetrical cell with $BaCO_3$ infiltrated SBF electrode measured under different oxygen partial pressures at 700 °C.

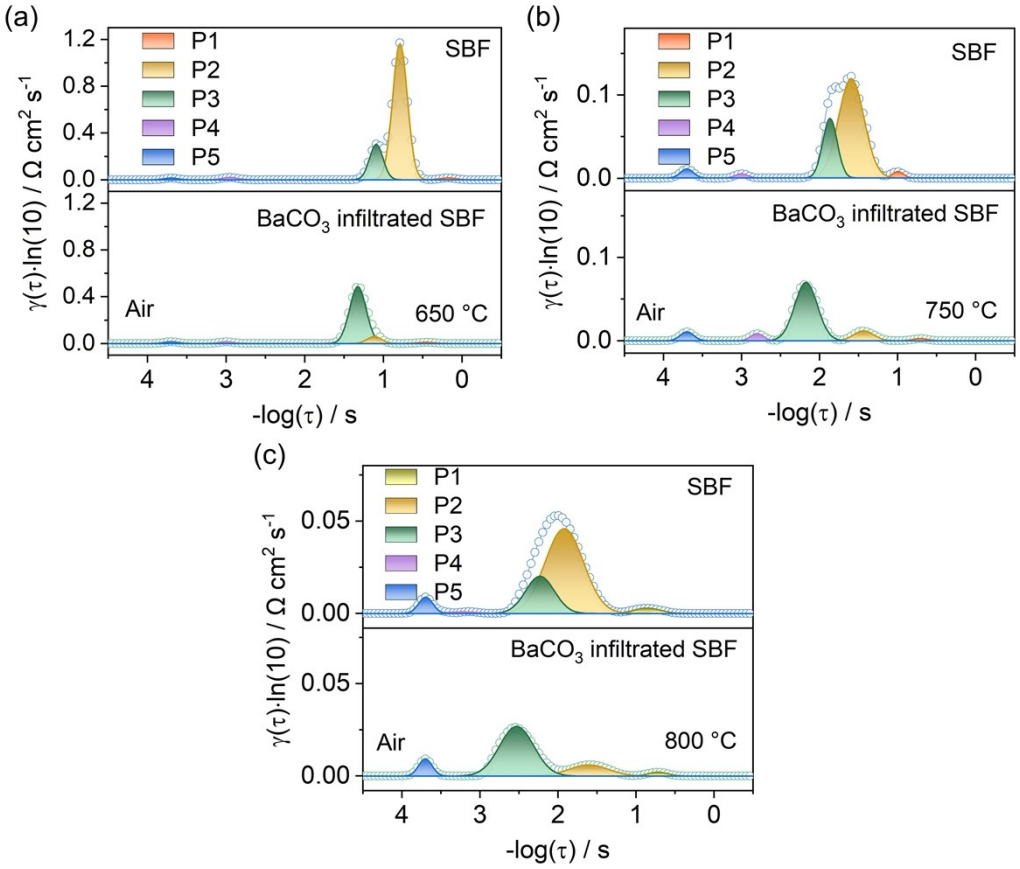

Fig. S7. DRT spectra of bare SBF and $BaCO_3$ infiltrated SBF electrode in air at 650 °C (a), 750 °C (b), and 800 °C (c).

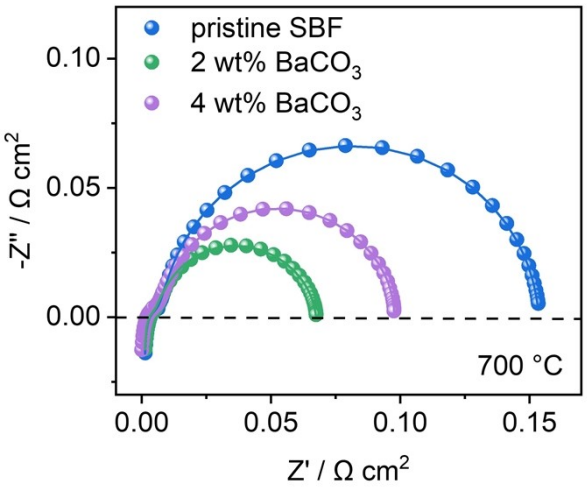

Fig. S8. Nyquist plots of symmetrical cell with SBF, 2 wt% and 4 wt% $BaCO_3$ infiltrated SBF electrodes measured in air at 700 °C.

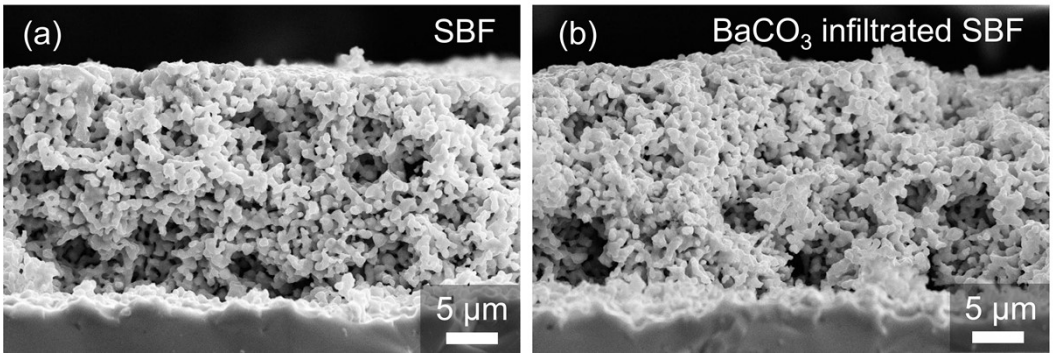

Fig. S9. Microstructure of cross-section of SBF (a) and $BaCO_3$ infiltrated SBF (b) electrodes.

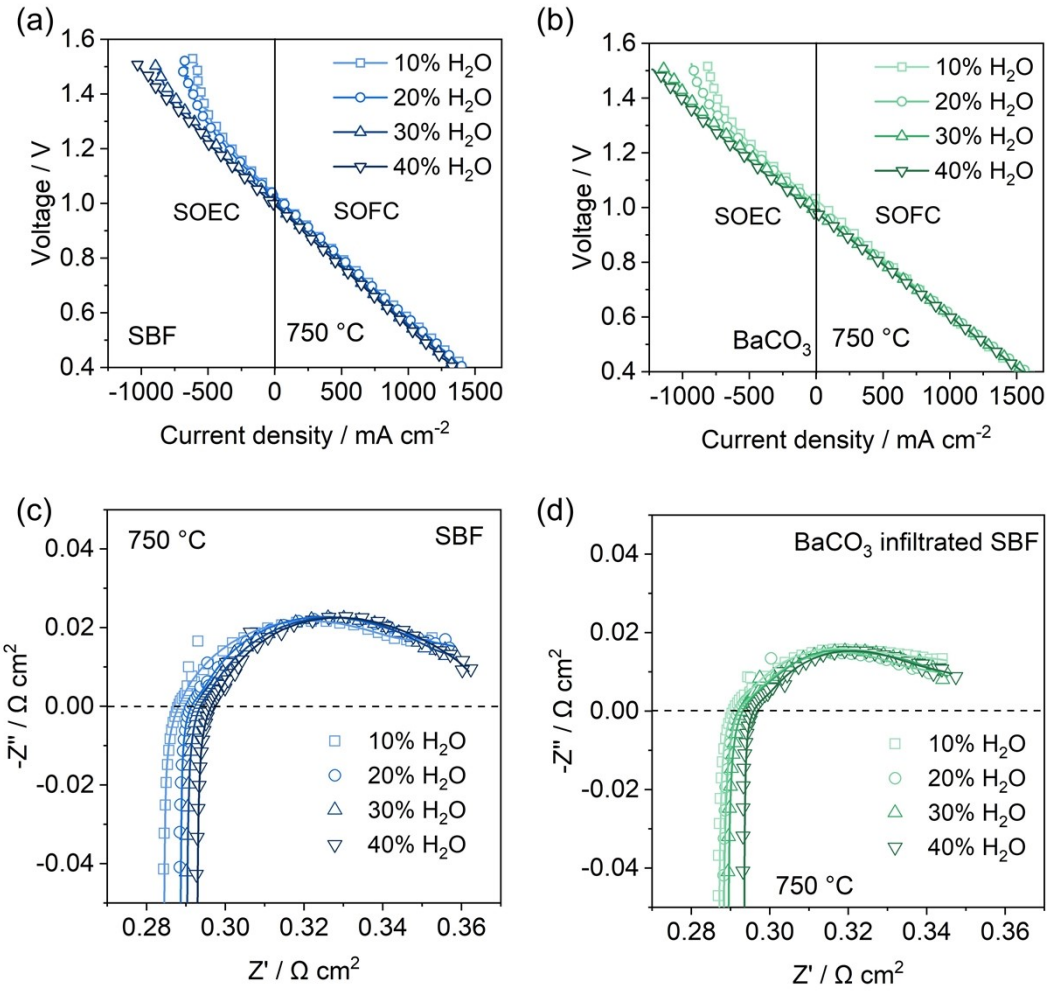

Fig. S10. Typical *I-V* curves of single cells of Ni-GDC|LDC|LSGM|SBF (a) and Ni-GDC|LDC|LSGM|$BaCO_3$ infiltrated SBF (b) at 750 °C with different humidity. EIS of single cells based on SBF (a) and $BaCO_3$ infiltrated SBF (b) air electrode under open-circuit conditions.

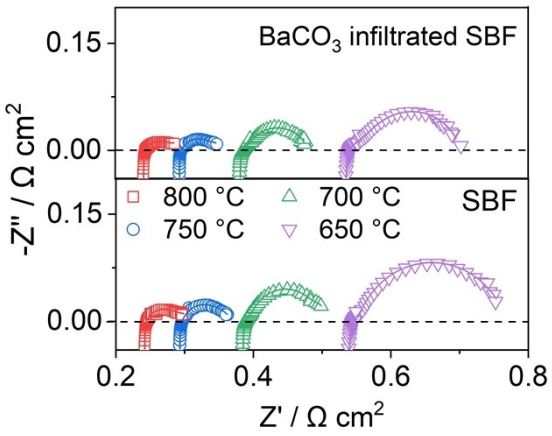

Fig. S11. EIS of single cells based on SBF and $BaCO_3$ infiltrated SBF air electrode with 40% H_2O/H_2 at fuel side under open-circuit condition.

Table S1. Rietveld refinement results of XRD data of synthesized SBF powders with different symmetries*.

Structure	*a* / Å	*b* / Å	*c* / Å	V / Å^3	χ^2	R_p / %	R_{wp} / %
Pmmm	3.9320(1)	3.9315(1)	7.8434(3)	121.249(8)	1.989	9.39	11.69
P4/mmm	3.92859(7)		7.8717(2)	121.491(6)	1.721	7.96	9.97

* Atoms Wyckoff position with *Pmmm* space group: Ba 1a (0, 0, 0); Sm 1c (0, 0, 0.5); Fe 2t (0.5, 0.5, *z*); O 1f (0.5, 0.5, 0); O2 2s (0.5, 0, *z*); O3 2r (0, 0.5, *z*); O4 1h (0.5, 0.5, 0.5).

Atoms Wyckoff position with *P4/mmm* space group: Ba 1a (0, 0, 0); Sm 1b (0, 0, 0.5); Fe 2h (0.5, 0.5, *z*); O 1c (0.5, 0.5, 0); O2 4i (0.5, 0, *z*); O3 1d (0.5, 0.5, 0.5).

Table S2. Comparison of the polarization resistance of air electrodes at 700 °C.

Materials	R_p / Ω cm^2	Reference
$La_{0.5}Sr_{0.5}Fe_{0.9}Mo_{0.1}O_{3-\delta}$	~0.21	1
$La_{0.5}Sr_{0.5}Fe_{0.8}Cu_{0.15}Nb_{0.05}O_{3-\delta}$	~0.35	2
$La_{0.6}Sr_{0.3}Ce_{0.1}Fe_{0.9}Ni_{0.1}O_{3-\delta}$	~0.26	3
$Sr_{0.95}Ti_{0.3}Fe_{0.6}Ni_{0.1}O_{3-\delta}$	~0.24	4
$Pr_{0.4}Sr_{0.5}Co_{0.7}Fe_{0.2}Mo_{0.1}O_{3-\delta}$	0.22	5
$PrBaFe_{1.9}Zr_{0.1}O_{5+\delta}$	0.134	6
$PrBaFe_{1.9}Zn_{0.1}O_{5+\delta}$	~0.17	7
$PrBaFe_{1.9}Ga_{0.1}O_{5+\delta}$	0.189	8
$SmBaFe_2O_{5+\delta}$	**0.154**	**This work**
$BaCO_3$ infiltrated $SmBaFe_2O_{5+\delta}$	**0.068**	**This work**

Table S3. Gibbs free energy of reaction $BaCO_3(s) = BaO(s) + CO_2(g)$ at different temperatures.

Temperature / °C	Gibbs free energy / kJ
650	54.17
700	42.89
750	31.69
800	20.60
900	0.09

Table S4. Fitted R_p values of elementary reactions of SBF and $BaCO_3$ infiltrated SBF electrodes with symmetrical cell configuration in air.

Temperatur	SBF / Ω cm^2					$BaCO_3$ infiltrated SBF/ Ω cm^2				
e / °C	P1	P2	P3	P4	P5	P1	P2	P3	P4	P5
650	0.0033	0.274	0.076	0.004	0.003	0.0025	0.0138	0.129	0.003	0.003
700	0.0015	0.089	0.050	0.003	0.003	0.0007	0.0050	0.057	0.002	0.003
750	0.0014	0.052	0.018	0.002	0.002	0.0006	0.0039	0.027	0.002	0.002
800	0.0012	0.028	0.009	0.0004	0.002	0.0006	0.0038	0.014	-	0.002

Reference

1 M. Wu, H. Cai, F. Jin, N. Sun, J. Xu, L. Zhang, X. Han, S. Wang, X. Su and W. Long, *J. Eur. Ceram. Soc.*, 2021, **41**, 2682-2690.

2 N. Zhou, Y.-M. Yin, J. Li, L. Xu and Z.-F. Ma, *J. Power Sources*, 2017, **340**, 373-379.

3 L. Z. Bian, L. J. Wang, N. Chen, F. S. Li and K.-C. Chou, *Ceram. Int.*, 2017, **43**, 982-987.

4 W. Ni, T. Zhu, X. Chen, Q. Zhong and W. Ma, *J. Power Sources*, 2020, **451**.

5 P. Li, Y. Han, M. Xu, T. Jin, F. Yan, T. Gan and R. Wang, *Energy Fuels*, 2022, **36**, 15165-15176.

6 G. Li, Y. Gou, X. Cheng, Z. Bai, R. Ren, C. Xu, J. Qiao, W. Sun, Z. Wang and K. Sun, *ACS Appl. Mater. Interfaces*, 2021, **13**, 34282-34291.

7 R. Ren, Z. Wang, X. Meng, C. Xu, J. Qiao, W. Sun and K. Sun, *ACS Appl. Mater. Interfaces*, 2020, **12**, 23959-23967.

8 B. Zhang, S. Zhang, H. Han, K. Tang and C. Xia, *ACS Appl. Mater. Interfaces*, 2023, **15**, 8253-8262.